Optical Nonlinearity Investigation of the Novel Organic-Inorganic Hybrid Salt: $1,1'$-methylenedipyridinium pentacynidonitrosoferrate(II)pentahydrate Using Z-Scan System

M.D. Zidan[a,*], M.M. Al-Ktaifani[b] and A. Allahham[a]

[a]Department of Physics,

[b]Department of Radioisotopes, Atomic Energy Commission, P.O. Box 6091, Damascus, Syria

The organic-inorganic hybrid salt: $1,1'$-methylenedipyridinium pentacynidonitrosoferrate(II)pentahydrate is synthesized and characterized by multinuclear NMR, IR, and UV-vis spectroscopies and elemental analysis. The third order nonlinear optical properties of the new complex in an aqueous solution have been studied using Z-scan technique. Measurements were performed for input intensities (I_0) of 437 and 241 W/cm^2 for the two concentrations with a CW diode laser at 635 nm wavelength. The nonlinear optical absorption coefficient (β) and nonlinear refraction (n_2) are found at 1.28×10^{-3} cm/W and 10.17×10^{-9} cm^2/W, respectively. The overall results suggested that better nonlinearity was observed at a higher concentration of sample. Our results suggest that this material is considered as a promising candidate for future optical device applications.

1. Introduction

Nonlinear optical (NLO) materials have been extensively studied for their potential applications in the protection of human eyes and solid-state optical sensors from high intensity laser beams [1–3]. A variety of organic materials have been investigated for NLO properties and optical limiting, such as: organic molecules [4–6], organic dyes [7], metallophthalocyanine [8] and fullerenes molecules and their derivatives [9, 10].

Special kind of π-conjugated organometallic complexes has attracted attention as promising third-order NLO materials [11–14]. These materials, which contain transition metal ions, exhibit new properties due to the richness of the various excited states present in the system and the ability to tailor the metal-organic ligand interactions. Furthermore, the delocalization of π-electron and the transfer of electron between the metal atom and the ligands make these complexes exhibit large third order NLO coefficients.

The proposed Z-scan method by Sheik-Bahae et al. [15, 16] was applied as a standard technique for separate determination of the nonlinear changes in refractive index and absorption. This method is sensitive to all nonlinear optical mechanisms that give rise to a change of the refractive index and absorption coefficient. Although number of organo-metallic complexes have been reported [17–22], using Z-scan technique, the investigation of organic-inorganic hybrid salts is limited [23], especially to third order NLO properties.

The aim of this article is to present the synthesis, characterization, and investigation of the third-order NLO properties of the novel organic-inorganic hybrid salt: $1,1'$-methylenedipyridinium pentacynidonitrosoferate(II)pentahydrate in aqueous solution using Z-scan technique at 635 nm wavelength.

2. Experimental techniques

2.1. Materials and methods

All reactions and manipulations were carried out in air with reagent grade solvents. $[(C_5H_5N)_2CH_2]Cl_2 \cdot H_2O$ was prepared according to literature method [24]. $Na_2[Fe(CN)_5NO] \cdot 2H_2O$ was purchased from Merck and used as received. The Fourier transform infrared (FTIR) spectrum was recorded on Thermo-Nicolet 6700 FTIR spectrometer taken as KBr disc with a resolution of 4 cm^{-1}. ^{1}H and ^{13}C$\{^1$H$\}$ nuclear magnetic resonance (NMR) spectra were acquired on a Bruker Bio spin 400 spectrometer. Microanalysis was performed using EURO EA. The ultraviolet-visible (UV-vis) absorption spectrum was recorded in the wavelength range 250–600 nm using UV-3101 PC Shimadzo spectrophotometer.

2.2. Synthesis of $1,1'$-methylenedipyridinium pentacynidonitrosoferate(II)pentahydrate

A solution of $[(C_5H_5N)_2CH_2]Cl_2 \cdot H_2O$ (0.40 g, 1.53 mmol) in H$_2$O (3 ml) was added to a solution of $Na_2[Fe(CN)_5NO] \cdot 2H_2O$ (0.45 g, 1.53 mmol) in H$_2$O (3 ml) at room temperature and stirred for overnight. The mixture was then left aside for two days to give brown powder, which was separated, washed with Et$_2$O and dried to afford an earth brown powder (0.5 g, yield 70%, at melting point 200 °C starts to decompose.).

———

[*]corresponding author; e-mail: pscientific@aec.org.sy

2.3. Spectroscopic data

The spectroscopic NMR data are the following:

- ^{1}H NMR (400 MHz, D_2O, 25 °C): $\delta = 7.34$ (s, 2H, CH_2), 8.24 (m, 4H, Py), 8.76 (m, 2H, Py), 9.24 (m, 4H, Py).

- $^{13}C\{^1H\}$ NMR: $\delta = 80.91$ (s, CH_2), 132.56 (s, Py), 148.06 (s, Py), 152.87 (s, Py), 136.91 (*cis*-C≡N), 134.69 (*trans*-C≡N).

- IR(KBr): ν cm^{-1}: 2146.1 (C≡N), 1920.5 (NO).

- UV(H_2O): $\lambda_{\max}(\varepsilon) = 218.0$ (1.014), 257.5 (0.642).

2.4. Analytical data

The analytical data are as follows:

- $C_{16}H_{22}N_8O_6Fe$ (487.24); C 41.04 (calc. 40.18); H 5.20 (4.64); N 23.29 (23.43).

2.5. Z-scan measurements

The Z-scan experimental setup was analogous to that described in Refs. [6, 25]. The measurements were done with linearly polarized TEM$_{00}$ Gaussian beam of a CW diode laser at maximum power of 26 mW ($\lambda = 635$ nm). The experimental parameters during the measurements of the samples were used as follows: the laser beam is focused by a 10 cm focal length lens to a waist radius (ω_0) of 33.5 μm at the focal point. The diffraction length (the Rayleigh length) z_0 is 5.5 mm, the radius of the aperture is $r_a = 0.5$ mm and the radius of the laser beam waist is $\omega_a = 7$ mm on the aperture at far field. The studied samples were dissolved in water with two concentrations of 5×10^{-3} M and 5×10^{-4} M. The sample cell used in this work is a 2 mm thick quartz cell and the cell was held on an optical rail and translated across the focal region along the axial direction that is in the direction of the propagation of the laser beam. The power transmitted through the sample is measured as a function of the sample distance z from the waist plane of the Gaussian beam. The transmission of the beam through an aperture placed in the far field is measured with a power meter (Thorlabs PM300E).

3. Results and discussion

3.1. NMR, FTIR, and UV-vis characterizations

The obtained product was purely isolated as an earth brown powder and characterized by multi-nuclear NMR, FTIR, UV-vis absorption spectra and elemental analysis (see Sect. 2). The spectroscopic data are very informative and quite consistent with the molecular structure of the product (Fig. 1).

The FTIR spectrum (Fig. 2) shows the characteristic band at 2146.3 cm^{-1}, which is readily assigned to the CN groups [26], while the distinctive absorption band at 1920.5 cm^{-1} is characteristic of Fe–NO group. Furthermore, the relatively high absorption frequency of the nitrosyl group (in the range 1650–1900 cm^{-1}) indicates that NO is coordinated to the Fe center in a linear geometry [27]. The ^{1}H NMR spectrum shows the expected
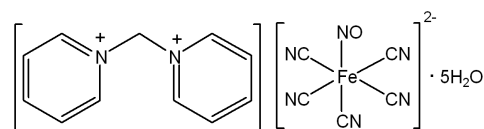

Fig. 1. Molecular structure of $1,1'$-methylenedipyridinium pentacynidonitrosoferrate(II)pentahydrate.
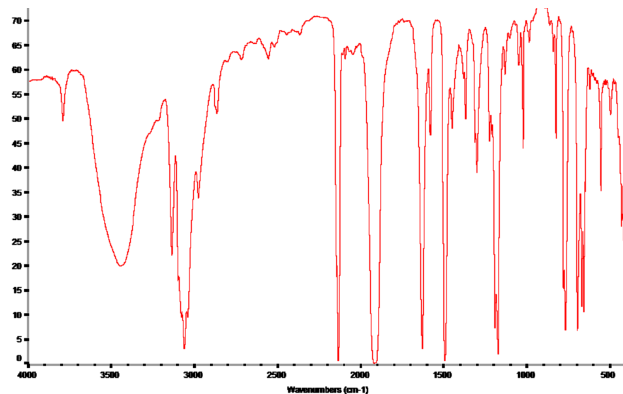

Fig. 2. FTIR spectrum of $1,1'$-methylenedipyridinium pentacynidonitrosoferrate(II)pentahydrate (KBr disc).

four resonances for four different proton groups at 7.34 (singlet) representing the CH_2 while the three resonances at 8.24, 8.76, and 9.24 ppm correspond to three environmentally different proton groups of pyridine. The ^{1}H NMR peaks are in their expected intensity ratio. The $^{13}C\{^1H\}$ NMR spectrum gives six singlets for six environmentally different C centers, three peaks at 132.56 (CH_2), 148.06, and 152.87 ppm represent the C nuclei of the pyridine rings, while two peaks at 134.69 and 136.91 ppm are observed for the two environmentally different CN groups. One (low intensity) CN group is in the *trans*-position, while the second (high intensity) represents four C≡N groups in the *cis*-positions to the nitrosyl group of [Fe(CN)$_5$NO]. It is worth mentioning, except the extra peaks associated with [Fe(CN)$_5$NO] moiety of the product, its IR, ^{1}H and $^{13}C\{^1H\}$ NMR spectra have the same features to their corresponding ones of the related structurally characterized organic-inorganic hybrid salts [(C$_5$H$_5$N)$_2$CH$_2$][MCl$_4$] (M = Zn, Cd, Pt or Cu) [28–30].

The UV-vis absorption spectrum of the product (Fig. 3) shows two maximum absorption peaks at 257.5(2.40) and 218.0(1.8) nm, which are readily attributed to $\pi \rightarrow \pi^*$ transition within the $1,1'$-methylenedipyridinium dication and ligand–metal charge transfer transitions (LMCT) and/or any $d \rightarrow d^*$ transition of the anionic fragment, respectively.

3.2. Nonlinear measurements

In the present investigation, Z-scan experiments were performed in order to determine the nonlinear absorption coefficient β and the nonlinear refractive index n_2 of the $1,1'$-methylenedipyridinium pentacynidonitrosoferate(II)pentahydrate in aqueous solution at two concentrations of 5×10^{-3} M and 5×10^{-4} M for input intensities
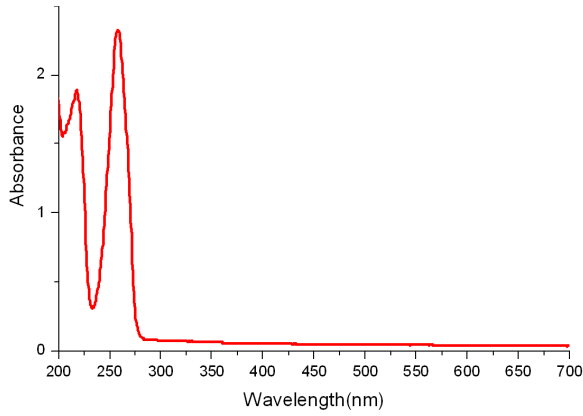
Fig. 3. UV-vis spectrum of $1,1'$-methylenedipyridinium pentacynidonitrosoferrate(II)pentahydrate in water.
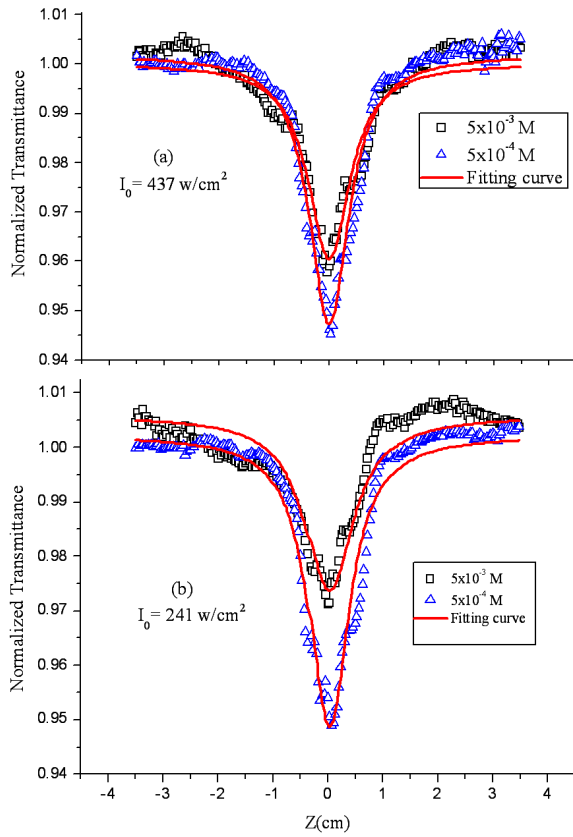

Fig. 4. Open-aperture Z-scan data of $1,1'$-methylenedipyridinium pentacynidonitrosoferrate(II)-pentahydrate in water for input intensities of (a) $I_0 = 437$ W/cm^2 and (b) $I_0 = 241$ W/cm^2 at two concentrations of 5×10^{-3} M and 5×10^{-4} M.

of $I_0 = 437$ W/cm^2 and 241 W/cm^2 for the two concentrations.

The open-aperture and closed-aperture of the Z-scan transmittance curves of the samples solutions were shown in Figs. 4 and 5, respectively. In the open-aperture Z-scan measurements ($S = 1$), when the sample is moved from negative z to focus ($z = 0$), initially the laser beam
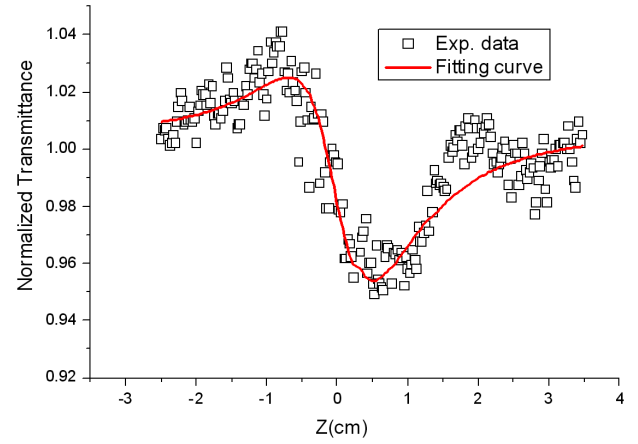

Fig. 5. Closed-aperture Z-scan data of $1,1'$-methyl-enedipyridinium pentacynidonitrosoferrate(II)penta-hydrate in water for $I_0 = 437$ W/cm^2 at concentration of 5×10^{-3} M.

intensity is low and the normalized transmittance is close to one. When the samples move closer to the focus, the laser beam intensity increases, leading to thermal-lensing effect in the sample media. The transmittance curves obtained are symmetric about focus for all sample concentrations, as shown in Fig. 4a,b. This characteristic indicates that our sample exhibits thermal induced nonlinearity due to the nonlinear absorption processes [16, 31, 32]. The nonlinear absorption in such materials arises from multiphoton absorption processes.

Figure 5 shows the closed-aperture data of the $1,1'$-methylenedipyridinium pentacynidonitrosoferrate(II)-pentahydrate in aqueous solution at concentration of 5×10^{-3} M. The experimental data show that $1,1'$-methylenedipyridinium pentacynidonitrosoferrate(II)-pentahydrate exhibits strong self-defocusing effect and negative sign of n_2 ($n_2 < 0$) as revealed in the obtained peak-valley shaped curve. The self-defocusing effect obtained in the studied sample is due to the local variation of the refractive index with the temperature ($\mathrm{d}n/\mathrm{d}T$), and is attributed to a thermal nonlinearity resulting from the incident tightly focused CW laser beam. The localized absorption of the laser beam propagating through an absorbing solution medium produces a spatial distribution of the temperature in sample solution and, consequently, a spatial variation of the refractive index that acts as a thermal lens results in the phase distortion of the propagating beam [25, 33, 34]. The thermal effect has been discussed by Sheik-Bahae et al. [15, 16, 35] in terms of temperature derivative of the index of refraction ($\mathrm{d}n/\mathrm{d}T$) of the medium.

The laser beam induced nonlinear absorption and nonlinear refraction change in Z-scan measurements. The nonlinear absorption coefficient β can be obtained from this open aperture Z-scan data by fitting the normalized transmittance data to the open aperture formula given as [15, 16] for $q_0 < 1$:

$$T(z) = \sum_{m=0}^{\infty} \frac{(-q_0)^m}{(m+1)^{\frac{3}{2}}}, \qquad (1)$$

where $q_0(z)$ is a parameter function of I_0, L_{eff}, and β:

$$q_0(z) = I_0 L_{\text{eff}} \beta / (1 + z^2/z_0^2),$$

where $L_{\text{eff}} = [1 - \exp(-\alpha_0 L)]/\alpha_0$ is the effective thickness of the sample, L is the thickness of the sample, α_0 is the linear absorption coefficient.

Solving the summation (1) and for $\alpha_0 \ll 1$:

$$T(z) = 1 - I_0 L \beta / [2^{3/2}(1 + z^2/z_0^2)], \qquad (2)$$

where $z_0 = \pi \omega_0^2/\lambda$ is diffraction length of the beam, λ is the laser wavelength, ω_0 is the laser beam waist radius at the focal point and I_0 is the intensity of the laser beam at focus $z = 0$. The solid lines in Fig. 4 are the fitting curves using Eq. (2), while the symbols are for the experimental data. The depth of the valley in open aperture Z-scans (Fig. 4) should be changed linearly after varying the intensity of the laser beam by nearly a factor of 2 ($I_0 = 241$ W/cm^2 and $I_0 = 437$ W/cm^2). But, at the lower concentration of 5×10^{-4} M and $I_0 = 241$ W/cm^2, this did not follow the linear behavior.

To determine the sign and magnitude of nonlinear refractive index n_2 of the studied sample, the normalized transmittance of closed aperture is given by [16, 35–37]:

$$T(z, \Delta\varphi) = 1 - \frac{4X}{(X^2 + 9)(X^2 + 1)} \Delta\varphi_0, \qquad (3)$$

where $X = z/z_0$ and $\Delta\varphi_0$ is on-axis nonlinear phase shift. The normalized closed aperture Z-scan data are fitted with Eq. (3) to obtain $\Delta\varphi_0$ values. The nonlinear refractive index n_2 is related to $\Delta\varphi_0$ by Eq. (4):

$$n_2 = \frac{\lambda \Delta\varphi_0}{2\pi I_0 L_{\text{eff}}}. \qquad (4)$$

The variation between the normalized peak and valley transmission T_{p-v} as function of $\Delta\varphi_0$ is given by

$$\Delta T_{p-v} = 0.406(1-S)^{0.25}|\Delta\varphi_0|, \qquad (5)$$

where S is the linear aperture transmittance $S = 1 - \exp(-2r_a^2/\omega_a^2)$, r_a is the radius of the aperture and ω_a is radius of the laser beam waist.

Also, the nonlinear refractive index n_2 of the studied samples can be obtained experimentally from Fig. 5 by measuring T_{p-v} and using Eqs. (4) and (5).

The calculated value of n_2 may have contributions of distinct origins, such as electronic (n_2^{e}) or thermal effects (n_2^{th}). Hence, one can separate such contributions by the relation [38]:

$$n_2 = n_2^{\text{e}} + n_2^{\text{th}}. \qquad (6)$$

The thermal nonlinearity n_2 is related with the thermo-optic coefficient $\mathrm{d}n/\mathrm{d}T$ by the

$$\left(\frac{\mathrm{d}n}{\mathrm{d}T}\right) = \frac{4n_2^{\text{th}}\kappa}{\alpha_0 w_0^2}, \qquad (7)$$

where $\kappa = 0.609$ W/(m K) and w_0 are the thermal conductivity and the radius of beam waist, respectively. All the calculated values of the n_2, β, and the thermo-optic coefficient $\mathrm{d}n/\mathrm{d}T$ of our samples have been estimated and listed in Table I.

From the nonlinear refractive index n_2 and nonlinear absorption coefficient β, the real and imaginary parts of the third-order nonlinear optical susceptibility (χ^3) were calculated according to the following relations [15, 16]:

$$\text{Re}\chi^3(\text{esu}) = (10^{-4}\varepsilon_0 c^2 n_0^2/\pi)n_2 \ [\text{cm}^2/\text{W}], \qquad (8)$$

$$\text{Im}\chi^3(\text{esu}) = (10^{-2}\varepsilon_0 c^2 n_0^2 \lambda/4\pi^2)\beta \ [\text{cm}/\text{W}], \qquad (9)$$

where ε_0 is the vacuum permittivity and c is the speed of light in vacuum.

Values of α_0 and n_0 were measured for the studied sample and shown in Table II. Value of α_0 was measured using a CW diode laser ($\lambda = 635$ nm) at low incident power. The output power varies linearly with incident power, the transmittance obeyed the Beer law: $I = I_0 e^{-\alpha 0L}$, where I, I_0, α_0 and L are the output power, the incident power, the linear absorption coefficient, and the sample path length, respectively. An Abbe refractometer is used for measurement of the linear refractive index (n_0).

TABLE II

The measured values of linear refractive index n_0 and linear absorption coefficient α_0 of 1,1'-methylenedipyridinium pentacynidonitroso-ferrate(II)pentahydrate in aqueous solution at two concentrations of 5×10^{-3} M and 5×10^{-4} M.

Concentrations	α_0 [cm^{-1}]	n_0
5×10^{-3} M	0.67	1.3315
5×10^{-4} M	0.46	1.3339

TABLE I

The calculated nonlinear optical parameters of 1,1'-methylenedipyridinium pentacynido-nitrosoferrate(II)pentahydrate in aqueous solution for input intensities of $I_0 = 437$ W/cm^2 and 241 W/cm^2 at two concentrations of 5×10^{-3} M and 5×10^{-4} M.

Concentrations	$\mathrm{d}n/\mathrm{d}T$ [μK^{-1}]	I_0 [W/cm^2]	$n_2 \times 10^{-9}$ [cm^2/W]	$\beta \times 10^{-3}$ [cm/W]	Re(χ^3) $\times 10^{-7}$ [esu]	Im(χ^3) $\times 10^{-5}$ [esu]
5×10^{-3} M	32.9	437	10.17	1.28	4.57	2.91
	241	64.8	20.03	1.87	9	4.25
5×10^{-4} M	437	45.7	9.7	1.11	4.37	2.53
	47.6	241	10.1	1.89	4.55	4.31

Concentration dependence effect was investigated and shown in Fig. 4. It is indicated that the nonlinear absorption coefficient (β) and nonlinear index of refraction (n_2) are functions of concentrations of the samples. It has been found that the β and n_2 values increase with an increase in concentration of the samples (Table I). This may be attributed to the fact that the number of molecules participating increases with an increase in concentration and more number of particles are thermally agitated, resulting in an increase in third-order optical nonlinearity [39]. From Table I it is clear that β and n_2 decrease with an increase in the intensity which is produced as a result of thermal nonlinear process [40]. This indicates that the thermal effect becomes more prominent at lower beam intensity.

The obtained values of β, n_2, $|\mathrm{Re}\chi^3|$ and $|\mathrm{Im}\chi^3|$ of the studied samples were determined using the fitting curves of the open/closed aperture measurements (Figs. 4 and 5) and Eqs. (1)–(7), and shown in Table I. The errors in estimating these values (Table I) arise from the uncertainties in the measuring of the focal spot size ($\pm 5\%$), linear refractive index ($\pm 0.3\%$), linear absorption coefficient ($\pm 5\%$) and the Rayleigh length ($\pm 4\%$). The maximum error in such measurements should be less than 5% for each parameter.

The reported values of n_2 and β of the studied sample in Table I can be compared with recently reported values of n_2 and β of different nonlinear optical materials with CW laser excitation [19, 41–44].

It can be seen that 1,1′-methylenedipyridinium penta-cynidonitrosoferrate(II)pentahydrate shows large third-order nonlinear optical properties because of the delocalized electronic states formed by the overlapping between $\pi \to \pi^*$ and d orbitals [19, 44, 45].

The experiments were repeated for the pure solvent to account for its contribution, but no significant measurable signals were produced in either the opened or the closed Z-scan traces. Also, it was found that the time employed for recording the Z-scan data in each plot does not affect the results for evaluating the nonlinear coefficients.

4. Conclusion

Synthesis, spectroscopic characterization, and the Z-scan measurements of 1,1′-methylenedipyridinium pentacynidonitrosoferrate(II)pentahydrate, using a CW diode laser at 635 nm wavelength have been presented. Depending on the experimental results, values of α_0, n_0, n_2, β, $\mathrm{Re}\chi^3$, $\mathrm{Im}\chi^3$, and the thermo-optic coefficient $\mathrm{d}n/\mathrm{d}T$ are calculated, and they are affected by the nature of attached ligand. It can be concluded that the combination of organic dication (with delocalized π-electron system) and inorganic anion (with π-electron system and d orbitals) in 1,1′-methylenedipyridinium pentacynido-nitrosoferrate(II)pentahydrate gives good optical nonlinearity. The studied sample exhibits self-defocussing property with a negative value of nonlinear refractive index.

References

[1] S.H. Nalwa, S. Miyata (Eds.), *Opt. Eng.* **36**, 2622 (1997).

[2] *Characterization Techniques and Tabulations for Organic Nonlinear Optical Materials*, Eds. M.G. Kuzyk, C.W. Dirk, Marcel Dekker, New York 1998.

[3] L.W. Tutt, T.F. Boggess, *Prog. Quant. Electron.* **17**, 299 (1993).

[4] B. Chandrakantha, A.M. Isloor, R. Philip, M. Mohesh, P. Shetty, A.M. Vijesh, *Bull. Mater. Sci.* **34**, 887 (2011).

[5] A.W. Allaf, M.D. Zidan, *Laser Phys.* **14**, 1529 (2004).

[6] M.D. Zidan, M. Al-Ktaifani, A. Allahham, *Opt. Laser Technol.* **70**, 45 (2015).

[7] S. Pramodini, P. Poornesh, *Opt. Laser Technol.* **63**, 114 (2014).

[8] T. Ceyhan, M. Yüksek, H. Gül Yağlıoğlu, B. Salih, M.K. Erbil, A. Elmalı, Ö. Bekaroğlu, *Dalton Trans.* **18**, 2407 (2008).

[9] H.I. Elim, J. Ouyang, J. He, S.H. Goh, S.H. Tang, W. Ji, *Chem. Phys. Lett.* **369**, 281 (2003).

[10] A.R. Kost, J.E. Jensen, R.O. Loufty, J.C. Wither, *Appl. Phys. B* **80**, 281 (2005).

[11] H. Fan, X. Wang, Q. Ren, X. Zhao, G. Zhang, J. Chen, D. Xu, G. Yu, Z. Sun, *Opt. Laser Technol.* **42**, 732 (2010).

[12] C. Yao, Y. Zhang, H. Yin, Q. Meng, C. Yu, J. Li, P. Yuan, *Chem. Phys. Lett.* **576**, 35 (2013).

[13] Y. Ji, J. Zuo, L. Chen, Y. Tian, Y. Song, Y. Li, X. You, *J. Phys. Chem. Solids* **66**, 207 (2005).

[14] Y. Cheng, Y. Mao, J. Liu, S. Feng, T. He, *J. Mod. Opt.* **54**, 2763 (2007).

[15] M. Sheik-Bahae, A.A. Said, E.W. Van Stryland, *Opt. Lett.* **14**, 955 (1989).

[16] M. Sheik-Bahae, A.A. Said, T. Wei, D.J. Hagan, E.W. Van Stryland, *IEEE J. Quant. Electron.* **QE-26** 760 (1990).

[17] K.B. Manjunatha, R. Dileep, G. Umesh, B. Ramachandra, *Mater. Lett.* **105**, 173 (2013).

[18] T.C. Sabari Girisun, S. Dhanuskodi, G. Vinitha, *Mater. Chem. Phys.* **129**, 9 (2011).

[19] H. Fan, Q. Ren, X. Wang, T. Li, J. Sun, G. Zhang, D. Xu, G. Yu, Z. Sun, *Nat. Sci.* **1**, 136 (2009).

[20] Q. Ren, X.B. Sun, X.Q. Wang, G.H. Zhang, X.D. Yang, F.J. Zhang, H.I. Yang, Y.T. Chow, D. Xu, *Appl. Phys. A* **90**, 685 (2008).

[21] J. Sun, W.F. Guo, X.Q. Wang, G.H. Zhang, X.B. Sun, L.Y. Zhu, Q. Ren, D. Xu, *Opt. Commun.* **280**, 183 (2007).

[22] Q. Chang, X. Meng, Y. Song, H. Hou, *Inorg. Chim. Acta* **358**, 2117 (2005).

[23] H. Li, Z. Chen, L. Cheng, J. Liu, X. Chen, J. Li, *Cryst. Growth Des.* **8**, 4355 (2008).

[24] B. Almarzoqi, A.V. George, N.S. Isaacs, *Tetrahedron* **42**, 601 (1986).

[25] M.D. Zidan, A.W. Allaf, M.B. Alsous, A. Allahham, *Opt. Laser Technol.* **58**, 128 (2014).

[26] W. Kemp, *Organic Spectroscopy*, 3rd ed., MacMillan Press Ltd, London 1991.

[27] C. De La Cruz, N. Sheppard, *Spectrochim. Acta Part A Mol. Biomol. Spectrosc.* **78**, 7 (2011).

[28] M.M. Al-Ktaifani, M.K. Rukiah, *Chem. Papers* **65**, 469 (2011).

[29] M.M. Al-Ktaifani, M.K. Rukiah, *Chem. Papers* **66**, 1032 (2012).

[30] M.M. Al-Ktaifani, M.K. Rukiah, *Acta Crystallogr. C* **68**, m246 (2012).

[31] I.A.H. Al-Saidi, S. Abdulkareem, *J. Mater. Sci. Mater. Electron.* **26**, 2713 (2015).

[32] U. Majitha Parvin, M. Basheer Ahamed, *Optik* **126**, 551 (2015).

[33] S. Zafar, Z.H. Khan, M.S. Khan, *Spectrochim. Acta Part A Mol. Biomol. Spectrosc.* **114**, 164 (2013).

[34] F.Z. Henari, W.J. Blau, *Proc. SPIE* **2854**, 174 (1996).

[35] F.L.S. Cuppo, A.M.F. Neto, S. L. Gömeze, P.P. Muhoray, *J. Opt. Soc. Am. B* **19**, 1342 (2002).

[36] F.Z. Henari, P.S. Patil, *Opt. Phot. J.* **4**, 182 (2014).

[37] M. Saravanan, T.C. Sabari Girisun, G. Vinitha, *J. Mat. Sci.* **51**, 3289 (2016).

[38] R.F. Souza, M.A.R.C. Alencar, C.M. Nascimento, M.G.A. da Silva, M.R. Meneghetti, J.M. Hickmann, *Proc. SPIE* **6323**, 63231T (2006).

[39] S. Pramodini, P. Poornesh, *Opt. Laser Technol.* **62**, 12 (2014).

[40] Cheng-Bao Yao, Yun-Dong Zhang, Jin Li, Deng-Tai Chen, Hai-Tao Yin, Chang-Qiu Yu, Ping Yuan, *Opt. Mater.* **37**, 80 (2014).

[41] S. Pramodini, P. Poornesh, Y.N. Sudhakar, M. Selva Kumar, *Opt. Commun.* **293**, 125 (2013).

[42] K.K. Nagaraja, S. Pramodini, A. Santhosh Kumar, H.S. Nagaraja, P. Poornesh, D. Kekuda, *Opt. Mater.* **35**, 431 (2013).

[43] S. Dhanuskodi, T.C. Sabari Girisun, S. Vinitha, *Curr. Appl. Phys.* **11**, 860 (2011).

[44] M.D. Zidan, M. Alktaifani, A. Allahham, *Optik* **126**, 1491 (2015).

[45] S. Wang, W. Huang, T. Zhang, H. Yang, Q. Gong, Y. Okuma, M. Horikiri, Y.F. Miura, *Appl. Phys. Lett.* **75**, 1845 (1999).